

## Dome C East radar: Preliminary analysis of echo statistics

M. F. MARCUCCI<sup>(1)</sup>, I. COCO<sup>(2)</sup>, S. MASSETTI<sup>(1)</sup>, S. LONGO<sup>(3)</sup>, D. BIONDI<sup>(1)</sup>,  
E. SIMEOLI<sup>(4)</sup>, A. MARCHAUDON<sup>(5)</sup>, A. KOUSTOV<sup>(6)</sup>, G. PALLOCCHIA<sup>(1)</sup>,  
G. CONSOLINI<sup>(1)</sup> and M. LAURENZA<sup>(1)</sup>

<sup>(1)</sup> *INAF, Istituto di Astrofisica e Planetologia Spaziali - Roma, Italy*

<sup>(2)</sup> *INGV, Sezione di Roma 2 - Roma, Italy*

<sup>(3)</sup> *CNR, Dipartimento Terra Ambiente - Roma, Italy*

<sup>(4)</sup> *CNR, Reti e Servizi Informativi - Roma, Italy*

<sup>(5)</sup> *IRAP - Toulouse, France*

<sup>(6)</sup> *University of Saskatchewan - Saskatoon, Canada*

received 28 December 2018

**Summary.** — Ionospheric echo occurrence rates for the Dome C East Super Dual Auroral Radar Network radar are presented with a focus on seasonal and solar cycle effects.

### 1. – Introduction

The Dome C East (DCE) radar, located at the Concordia research station (Antarctica), is one of the high-frequency (HF) radars of the Super Dual Auroral Radar Network (SuperDARN). The main objective of SuperDARN is to continuously monitor the ionospheric convection at sub-auroral, auroral and polar cap latitudes in both Northern and Southern Hemispheres [1].

In SuperDARN, the transmitted HF radio waves are backscattered from decameter electron density irregularities in the ionospheric E and F regions. These irregularities are stretched along the Earth's magnetic field lines and radio waves have to propagate almost perpendicular to the magnetic field in order the backscatter to be sufficiently strong. This is possible at HF because radio waves can refract significantly, depending on the background electron density in the ionosphere. SuperDARN radars transmit multi-pulse signals along 16 beam directions covering about 50° in azimuth. Each radar scan is 1 minute. The DCE radar started its operation in January 2013 and until December 2016 employed a unique mode of operation with switching the transmitting frequency between ~10 MHz and ~12 MHz at every next scan. The power, Doppler velocity, and spectral width of echoes received from various ranges are inferred through the autocorrelation function analysis of multi-pulse signals. Typically, SuperDARN echoes are detected only

from a fraction of ranges and beams. The ionospheric echo occurrence (EO) rate depends on HF radio wave propagation conditions (controlled by the electron density distribution along the wave path) and on the presence of irregularities created by various plasma instabilities (controlled by the electric field and electron density plasma gradients). The gradient-drift plasma instability is the most likely source of decameter ionospheric irregularities [1]. Here we present data on the EO rate for the DCE radar. The data are split according to a season of observations in order to show the extent to which the EO rates of DCE are affected by the solar illumination of the ionosphere. We also consider 2 separate periods of observations corresponding to high and low solar activity in order to reveal the solar cycle effect.

## 2. – DCE observations of ionospheric echoes

For the analysis, data for one-month intervals and several years of observations were considered to achieve significant data statistics. Eight intervals (each centered at the equinox or solstice on a specific season) were studied: the southern AUTUMN, WINTER and SPRING of the years 2013 and 2016 and the southern SUMMER of the Dec 2014 – Jan 2015 and Dec 2015 – Jan 2016 periods. The 2013 intervals and the Dec 2014 – Jan 2015 period are characterized by high solar activity, while during 2016 and the Dec 2015 – Jan 2016 period the solar activity is lower. Only ionospheric echoes for which the velocity error was lower than 200 m/s (these are useful measurements for convection studies) were counted. For each counted echo, its height (using the virtual height model of [2]) and Altitude Adjusted Corrected Geomagnetic (AACGM) coordinates were computed according to [3]. The counts were then gridded in  $1^\circ$  AACGM Lat  $\times$   $5^\circ$  AACGM Lon (20 min in magnetic local time, MLT) cells from  $-55^\circ$  to  $-87^\circ$  AACGM Lat. The EO rate was calculated as the ratio of the number of counted echoes to the total number of soundings available for in each cell. The stereographic maps of the EO rate in the AACGM Lat - MLT coordinates are presented in fig. 1 for each season. In fig. 1, the top row corresponds to the period of high solar activity while the bottom row corresponds to the period of lower solar activity.

From panels a) to d) of fig. 1, one can conclude that the EO rate is generally lower in SUMMER. This is because under extended periods of solar illumination (up to 24 hours) the plasma density gradients are smoothed out and no irregularities can be produced through the gradient-drift plasma instability [4, 5]. Another possible reason is an increased electron density in the D and E regions causing enhanced HF signal absorption [4, 5]. In WINTER, the EO rate is generally not high because the polar cap is in darkness for extended periods of time (up to 24 hours) causing low electron density and insufficient ionospheric refraction of HF radio waves so that the echoes cannot be detected even if the irregularities are present. The echo enhancement between 17 and 03 MLT from  $-75^\circ$  to  $-85^\circ$  AACGM Lat is very likely related to the effects of auroral precipitation. Despite the fact that the peak rate is observed at latitudes above  $-80^\circ$ , we expect an expansion of auroral precipitation and enhanced electric fields (for example, due to substorm activity) into the polar cap in this time sector. In SPRING and AUTUMN, the rates are overall larger as compared to WINTER and SUMMER. Similar result was reported in [6], and it was attributed to the presence of enhanced electric fields (supporting the gradient drift instability) related to the tilt of the Earth's magnetic dipole axis. The EO rates drop between 05 and 11 MLT. This effect can be related to darkness in the dawn sector [7]. Comparing the maps of panels a) to d) with the maps of panels e) to h), one can conclude that the patterns of the enhanced EO are the same for the

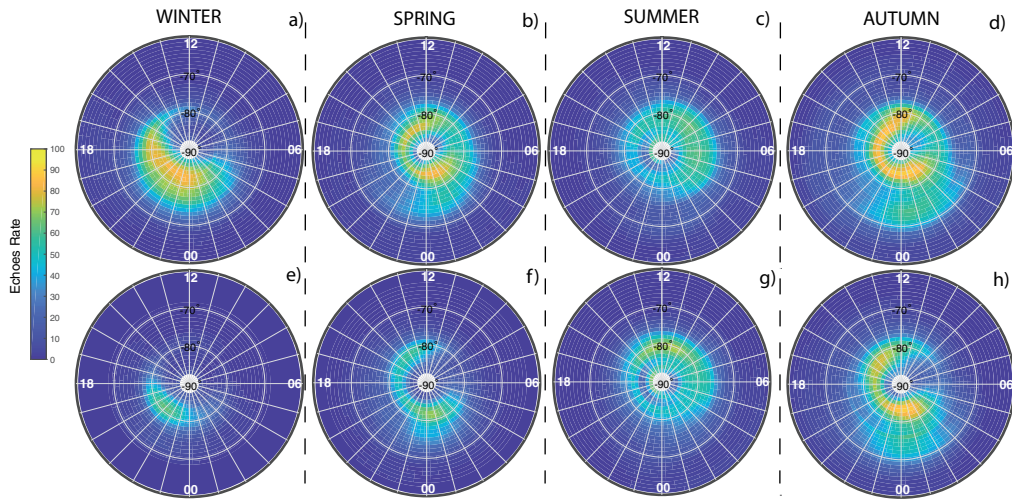


Fig. 1. – Echo occurrence rate (%) plotted in magnetic (AACGM) latitude - magnetic local time (MLT) coordinates. The maps of the top (bottom) row are for high (low) solar activity.

two datasets although the rate values are smaller for the lower solar activity condition. Similar result has been reported for the auroral zone radars [6]. The effect was related to general decrease in the intensity of electric fields affecting the irregularity creation.

### 3. – Conclusions

We made a preliminary analysis of ionospheric echo occurrence rates for the SuperDARN DCE radar by considering one month intervals of observations for various seasons at high (2013) and low solar activity (2016). We found, in agreement with previous reports, a strong seasonal dependence of echo occurrence related to changing HF radio wave propagation conditions and ionospheric irregularities development. Despite the overall agreement with previous observations with other SuperDARN radars, some peculiar features are evident in the DCE data, and these will be further investigated in a future work.

\* \* \*

This activity is supported by the Italian National Program for Antarctic Research.

### REFERENCES

- [1] CHISHAM G. *et al.*, *Surv. Geophys.*, **28** (2007) doi:10.1007/s10712-007-9017-8.
- [2] CHISHAM G., YEOMAN T. K., and SOFKO G. J., *Ann. Geophys.*, **26** (2008) 823-841.
- [3] SHEPHARD S., *J. Geophys. Res. Space Physics*, **119** (2014) doi:10.1002/2014JA020264.
- [4] RUHOUNIEMI J. R. and GREENWALD R. A., *Radio Science*, **32** (1997) doi:10.1029/97RS00116.
- [5] GHEZELBASH M. *et al.*, *J. Geophys. Res.*, **119** (2014b) doi:10.1002/2014JA020726.
- [6] KOUSTOV A. V. *et al.*, *J. Geophys. Res.*, **109** (2004) doi:10.1029/2003JA010337.
- [7] BRISTOW W. A. *et al.*, *J. Geophys. Res.*, **116** (2011) doi:10.1029/2011JA016834.